

1       **EFFECT OF AGING ON RHEOLOGICAL, CHEMICAL AND THERMODYNAMIC**  
2       **PROPERTIES OF ASPHALT COMPONENTS**

3  
4  
5       *Submitted to the 93<sup>rd</sup> Annual Meeting of the Transportation Research Board*  
6       Submitted on August 1, 2013  
7  
8  
9

10                   Fabricio Leiva-Villacorta Ph.D. (Corresponding Author)  
11           National Laboratory of Materials and Structural Models (LanammeUCR),  
12   University of Costa Rica, P.O.Box 11501-2060, UCR, San José, Costa Rica  
13                   fabricio.leiva@ucr.ac.cr  
14

15                   Rafael Ernesto Villegas-Villegas  
16           National Laboratory of Materials and Structural Models (LanammeUCR)  
17           University of Costa Rica, San José, Costa Rica  
18                   rafael.villegas@ucr.ac.cr  
19

20                   José Pablo Aguiar-Moya, Ph.D.  
21           National Laboratory of Materials and Structural Models (LanammeUCR)  
22           University of Costa Rica, San José, Costa Rica  
23                   jose.aguiar@ucr.ac.cr  
24

25                   Jorge Salazar-Delgado  
26           National Laboratory of Materials and Structural Models (LanammeUCR)  
27           University of Costa Rica, San José, Costa Rica  
28                   jorge.salazardelgado@ucr.ac.cr  
29

30                   Luis Guillermo Loría Salazar, Ph.D.  
31           National Laboratory of Materials and Structural Models (LanammeUCR)  
32           University of Costa Rica, San José, Costa Rica  
33                   luis.loriasalazar@ucr.ac.cr  
34  
35

36  
37       Word Count: Abstract (239) + Body (3,757) + Figures and Tables (14x250) = 7,496  
38

1 **ABSTRACT**

2  
3 Many molecular structures are found in asphalts; however, the commonly used classification  
4 separates asphalt into asphaltenes and maltenes (resins and oils). Rheology of asphalts depends on  
5 the combination of the different constitutive fractions and greatly depends on the degree of  
6 association of asphaltenes and the relative quantity of other substances present in the system to  
7 stabilize those associations. Asphalts are subjected to an aging process during mixing, laydown and  
8 service life that also affects their rheology. The objective of this study was to evaluate the effect of  
9 aging on rheological, chemical and thermodynamic properties of the asphalt binder main  
10 components: asphaltenes and maltenes. An AC-30 asphalt binder and its individual components  
11 were aged using the Rolling Thin Film Oven (RTFO) and the Pressure Aging Vessel (PAV), and  
12 were analyzed using a Dynamic Shear Rheometer (DSR). A Iatroscan thin film chromatography and  
13 a Polarized Light Microscopy analysis were also used for characterization purposes. A  
14 Thermogravimetric analysis (TGA), a Differential Scanning Calorimetry Analysis (DSC) and a  
15 Fourier Transform Infrared Spectroscopy (FTIR) analysis of the asphalt binder and its components  
16 were performed before and after aging. The results indicated that the thermal stability of the asphalt  
17 binder can be attributed mostly to the higher stability and lower susceptibility to oxidation of the  
18 asphaltenes at normal handling temperatures for paving operations. Overall, there is clear evidence  
19 that aging of the asphalt binder components has an effect on the morphology of the asphalt binder.

## 1 INTRODUCTION

2 Asphalt is a complex organic mixture, composed of hydrocarbons with small percentages of sulfur,  
3 nitrogen, and oxygen. Many molecular structures are found in asphalts; however, the commonly  
4 used classification separates asphalt into asphaltenes and maltenes (resins and oils). Asphaltenes are  
5 generally dark brown, friable solids and are the most complex components with the highest polarity.  
6 Resins are generally dark and semi-solid or solid in character. They are fluid when heated and  
7 become brittle when cold. On oxidation, resins yield asphaltene type molecules. Oils are usually  
8 colorless or white liquids. They have paraffinic and naphthenic structures with no oxygen and  
9 nitrogen usually present. On oxidation, they yield asphaltene and resin molecules (1).

10 Asphalt is most commonly modeled as a colloid (micellar model), with asphaltenes as the  
11 dispersed phase and maltenes as the continuous phase (2). The original micellar model was  
12 constructed from interpretations of historical data in which researchers looked for relationships  
13 between chemical parameters and pavement performance. According to this model, the rheology of  
14 the asphalt is highly affected by the degree to which the resins are effective in keeping the  
15 asphaltene fraction dispersed in the oil (3). Asphalts which have well-dispersed asphaltenes, exhibit  
16 high temperature susceptibilities, high ductility, low rates of age hardening, and Newtonian  
17 behavior. Asphalts which have poorly dispersed asphaltenes show low temperature susceptibilities,  
18 low ductility, rapid age-hardening, and non-Newtonian behavior (4).

19 Different effects on rheology of the binder can be obtained depending on how the different  
20 fractions are combined (5). For instance, if the content of asphaltenes is kept constant adding resins  
21 will produce a harder binder. The same hardening effect can be obtained by increasing the  
22 asphaltenes concentration into a maltenes constant structure. In addition, it is considered that at  
23 ambient and intermediate temperatures the rheology of asphalt binders is dominated by the degree  
24 of association of asphaltenes and the relative quantity of other substances present in the system to  
25 stabilize those associations.

26 Another factor influencing the rheology, performance and characteristics of asphalt binders  
27 is a phenomenon known as aging. Several factors may contribute to this hardening of the asphalt  
28 such as oxidation, volatilization, polymerization, and thixotropy (5-7). Because asphalt is an organic  
29 compound, it is able to react with oxygen in the environment. As the oxidation reaction occurs, it  
30 changes the composition of the asphalt, creating a more brittle structure. Volatilization occurs when  
31 the lighter constituents of the asphalt evaporate. Polymerization is the means by which resins are  
32 thought to combine into asphaltenes, causing an increase in the brittleness of the asphalt along with  
33 a tendency toward non-Newtonian behavior. Finally, thixotropy, or an decrease in viscosity over  
34 time, also contributes to the aging phenomenon in asphalt.

35 This report summarizes a comprehensive investigation on the effect of aging on chemical  
36 composition and rheological properties of asphalt binder components (asphaltenes and maltenes).

## 38 BACKGROUND

39  
40 To date, there is an increasing interest in understanding the micro-mechanical and chemical  
41 behavior of asphalt to better understand rheological properties and their effect on the performance  
42 of asphalt mixtures during their service life (8). Even though asphalt binder corresponds to a small  
43 percentage of the overall mixture volume, variations in the molecular distribution and micro-  
44 mechanical arrangement of the different components in asphalt binder, have a considerable impact  
45 in the performance of the mixture. This is due to the fact that small variations in the chemical and  
46 structural composition of the asphalt matrix have an effect on the rheological, viscoelastic and  
47 thermoplastic behavior of the material (8).

48

1           Techniques such as Thermogravimetric Analysis (TGA), Differential Scanning Calorimetry  
2 Analysis (DSC), Fourier Transformed Infrared Spectroscopy (FTIR) and Iatrosan thin film  
3 chromatography have been used to characterize the chemical composition and thermo dynamical  
4 behavior of the asphalt binder: Similarly, techniques such as the following can be used to analyze  
5 the micro-mechanical structure and behavior of the asphalt binder: dynamic shear rheometer (DSR),  
6 dynamic mechanical analyzer (DMA), atomic force microscopy (AFM), and electron microscopy.  
7 The previous techniques can also be used with thermal analysis to better understand the behavior of  
8 the material.

## 10 **OBJECTIVE**

12 The objective of this study was to evaluate the effect of aging on rheological, chemical and  
13 thermodynamic properties of the asphalt binder main components: asphaltenes and maltenes.

## 14 **SCOPE OF WORK**

15 To accomplish the objective of this study, the asphalt binder and its individual components  
16 (asphaltenes and maltenes) were aged using the Rolling Thin Film Oven (RTFO) and the Pressure  
17 Aging Vessel (PAV), and were also analyzed using a Dynamic Shear Rheometer. The binder was  
18 characterized using the Superpave methodology, based on the PG grading of the material and  
19 rheological properties were obtained for the same binder and its components at three aging stages or  
20 conditions (original, RTFO and PAV) and at two temperatures (25 °C and 64 °C). A Iatrosan thin  
21 film chromatography and a Polarized Light Microscopy analysis were also used for characterization  
22 purposes. A Thermogravimetric aTGA nalysis of the asphalt binder and its components was  
23 performed at the same three aging stages. A DSC Analysis was also performed to observe sample  
24 behavior due to the change on temperature in a range from -50°C up to 200°C at the same three  
25 aging stages. Finally, the Fourier Transform Infrared Spectrometry was used to determine the  
26 functional characteristics of the binder and its individual components before and after aging.

## 28 **CHARACTERIZATION OF THE BINDER AND ITS COMPONENTS**

29 The tests to characterize the bitumen and modifiers were performed at the National Laboratory for  
30 Materials and Structural Models (LanammeUCR, University of Costa Rica). The asphalt binder  
31 used in this study was classified as viscosity grade AC-30 provided by RECOPE (Costa Rican  
32 Petroleum Refinery). This grade corresponds to the most common binder used in Costa Rican roads.

### 34 **Iatrosan Chromatography**

36 A chromatography analysis made with the Iatrosan chromatographer showed that the fractions of  
37 the original (unaged) bitumen are distributed as follows: Saturated 5,2%, Aromatics 54.9%, Resins  
38 25.8% and Asphaltenes 14.1%. Figure 1 illustrates the binder fractions for the original and the  
39 RTFO and PAV aged binder . If compared to the original condition, the asphaltenes presented the  
40 lowest change in composition by decreasing 3.0 % at RTFO and 18% at PAV aging stage. On the  
41 other hand, resins' composition changed the most with an increase of 33 % at RTFO and 119% at  
42 PAV stage. It was also determined that aromatics are more likely to yield resin molecules on aging  
43 instead of yielding asphaltene molecules. In addition, there was no indication that resins yield  
44 asphaltene-like molecules on aging.

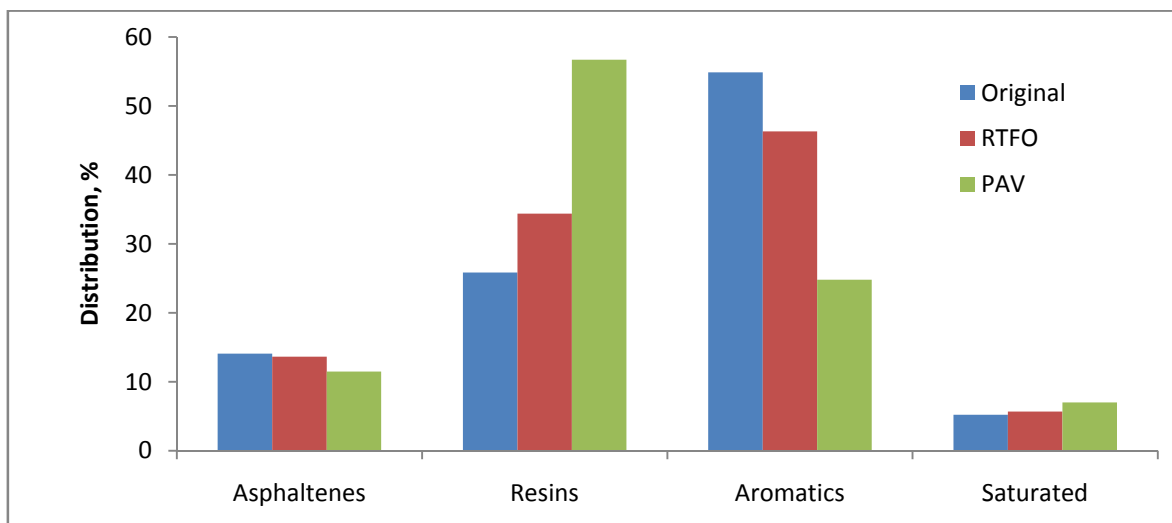


**FIGURE 1** Iatroscan Thin Film Chromatography analysis.

### Polarized Light Microscopy

Polarized light microscopy (PLM) is a useful method to determine qualitative and quantitative aspects of crystallographic axes and stress concentrations present in various materials (9). This technique can also distinguish between isotropic and anisotropic substances. It exploits the optical properties specific to anisotropy and reveals detailed information concerning the structure and composition of materials that are invaluable for identification purposes.

Figure 2 shows a PLM analysis of the binder, asphaltenes and maltenes. The variety of colors observed in the binder sample demonstrate the presence of different components. The green color observed in the asphaltene sample shows the highest stress concentration (harder material) of this component and the lighter colors observed in the maltene sample shows the lowest stress (softer) components. Figure 3 illustrates the effect of aging on the stress concentration of the samples. For instance, the red-brown tone almost disappeared at RTFO and PAV stages and the green (higher stress) tone started to show up, providing evidence that some of the resins and oils were transformed into asphaltene-like substances due to aging.



Original binder

Original Asphaltenes

Original Maltenes

**FIGURE 2** Polarized light microscopy analysis of original (unaged) samples

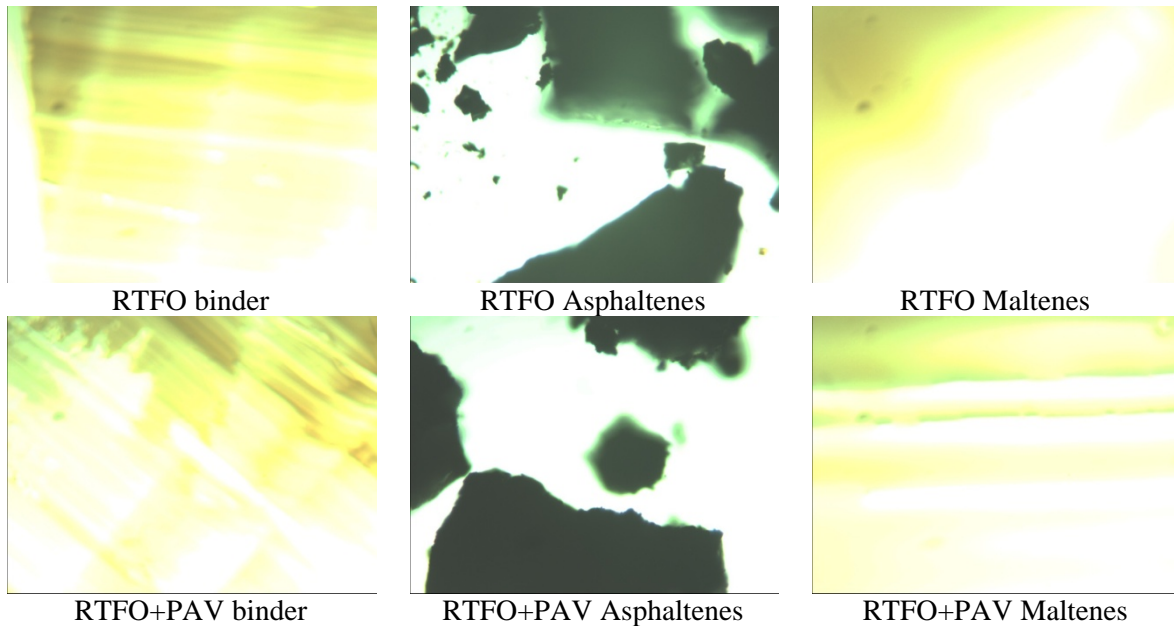


**FIGURE 3 Polarized light microscopy analysis of aged samples**

### RHEOLOGICAL CHARACTERIZATION

The binder characterization was performed following the Superpave methodology for the original bitumen, the short term aged bitumen (RTFO) and the long term aged bitumen (RTFO+PAV). The dynamic shear rheometer was used to measure the complex shear modulus ( $G^*$ ), storage modulus ( $G'$ ), the loss modulus ( $G''$ ) and phase angle ( $\delta$ ) of the binder samples in accordance to AASHTO T 315. Table 1 shows the Superpave characterization of the binder which resulted in a PG 64 with an intermediate temperature of 19 °C.

**TABLE 1 Performance Grade Results**

| Condition      | $ G^* $<br>(Pa) | $G'$<br>(Pa) | $G''$<br>(Pa) | $G''/G'$ | $\delta$ ,<br>degrees | $ G^* /\sin(\delta)$ |
|----------------|-----------------|--------------|---------------|----------|-----------------------|----------------------|
| Original 64 °C | 1974            | 164,6        | 1968          | 11.96    | 85.22                 | 1.981                |
| RTFOT 64 °C    | 5335            | 884,9        | 5261          | 5.95     | 80.45                 | 5.41                 |
| PAV 19 °C      | 6749000         | 5157000      | 4353000       | 0.84     | 40.17                 | 4353                 |

The binder used in this study was fractionated into two components - asphaltenes which correspond to 14.1% and maltenes which correspond to the remaining 85.9%. Table 2 shows the results of the DSR tests performed on the binder and the two individual components. In this case a 40 mm plate was used to obtain the complex shear modulus and phase angle. The testing was performed with the same plate for all the stages so the test could be performed on the maltenes and to be able to compare results under the same testing conditions. As expected, the results indicated that with aging the complex modulus, storage modulus and the loss modulus of the binder increase while the phase angle decreases. In other words, aging causes the mechanical properties of the asphalt binder to resemble those of a solid.

Also as expected, maltenes had lower  $G^*$  values, higher phase angles, higher  $G''/G'$  ratios and lower  $|G^*|/\sin(\delta)$  values than the asphalt binder since they account for the majority of the viscous component of the binder at 25 °C. On the other hand, for asphaltenes these four parameters had the opposite behavior compared to maltenes confirming that asphaltenes account for the majority of the elastic component of the binder at 25 °C. When testing at 64 °C a significant decrease in the  $G''/G'$  ratio and the phase angle of the maltenes was obtained for all three aging stages. This unexpected behavior was attributed, at this point, to the low viscosity of the maltenes at high temperatures and the limitation of the DSR plate to provide reliable results at such a low viscosity. On the other hand, asphaltenes started to perform more as viscous material with a  $G''/G'$  ratio over 1.0. Moreover, they showed a significantly higher phase angle which was closer to the angle obtained for the original binder at the same temperature.

**TABLE 2 Rheological analysis of the binder and its individual components**

| Condition                              | $ G^* $<br>(Pa) | $G'$<br>(Pa) | $G''$<br>(Pa) | $G''/G'$ | $\delta$ , degrees | $ G^* /\sin(\delta)$ |
|--|-----------------|--------------|---------------|----------|--------------------|----------------------|
| <b>Asphalt binder analysis at 25°C</b> |                 |              |               |          |                    |                      |
| Original                               | 469500          | 100600       | 458600        | 4.56     | 77.63              | 480.7                |
| RTFT                                   | 898500          | 306900       | 844400        | 2.75     | 70.03              | 956                  |
| PAV                                    | 1190000         | 735300       | 935000        | 1.27     | 51.82              | 1513                 |
| <b>Maltenes analysis at 25°C 25°C</b>  |                 |              |               |          |                    |                      |
| Original                               | 1465            | 198.6        | 1451          | 7.31     | 82.21              | 1.478                |
| RTFOT                                  | 683.1           | 174.5        | 660.5         | 3.79     | 75.2               | 0.7065               |
| PAV                                    | 427.9           | 147.7        | 401.6         | 2.72     | 69.81              | 0.4559               |
| <b>Asphaltenes analysis at 25°C</b>    |                 |              |               |          |                    |                      |
| Asphaltenes                            | 1358000         | 1350000      | 142500        | 0.11     | 6.025              | 12930                |
| <b>Asphalt binder analysis 64°C</b>    |                 |              |               |          |                    |                      |
| Original                               | 994.3           | 203.6        | 973.2         | 4.78     | 78.18              | 1.016                |
| RTFT                                   | 2986            | 624.1        | 2920          | 4.68     | 77.94              | 3.054                |
| PAV                                    | 9929            | 3241         | 9385          | 2.9      | 70.95              | 10.5                 |
| <b>Maltenes analysis at 64°C</b>       |                 |              |               |          |                    |                      |
| Original                               | 161.4           | 155.9        | 41.72         | 0.27     | 14.98              | 0.6243               |
| RTFOT                                  | 129.5           | 122.2        | 43.01         | 0.35     | 16.12              | 0.3901               |
| PAV                                    | 109.3           | 98.93        | 46.46         | 0.47     | 25.15              | 0.2571               |
| <b>Asphaltenes analysis at 64°C</b>    |                 |              |               |          |                    |                      |
| Asphaltenes                            | 19190           | 9906         | 16440         | 1.66     | 58.93              | 22.41                |

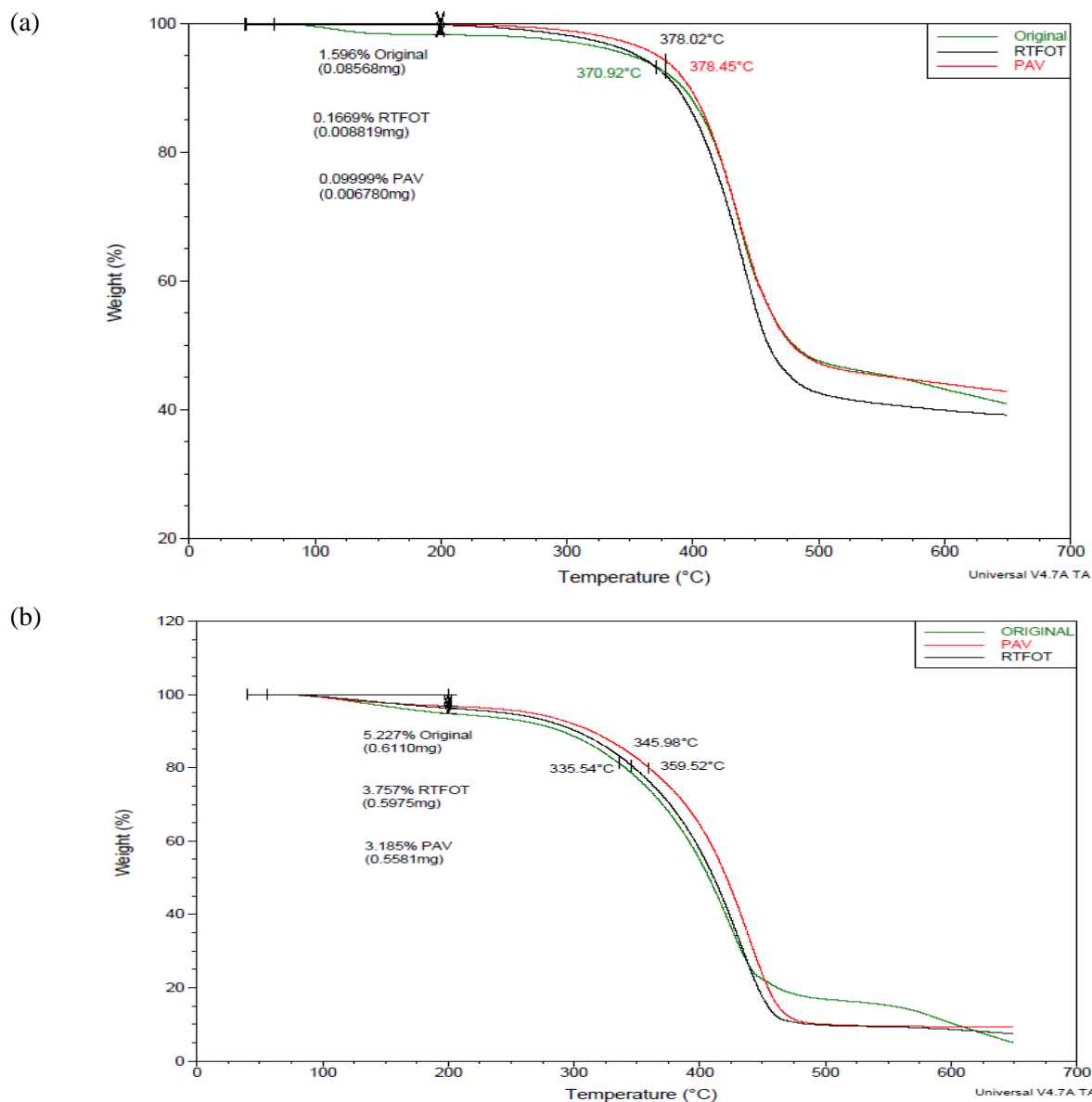
## THERMOGRAVIMETRIC ANALYSIS

TGA is a method of thermal analysis in which changes in physical and chemical properties of materials are measured as a function of increasing or decreasing temperature cycles (with constant heating rate), or as a function of time (with constant temperature and/or constant mass loss) (10). TGA is commonly used to determine selected characteristics of materials that exhibit either mass loss or gain due to decomposition, oxidation, or loss of volatiles. As shown in Figure 4, the mass loss of asphaltenes decreased when going from the original (unaged) stage to the highest aging

1 stage. Besides, the lowest temperature of decomposition was observed for the asphaltenes at the  
2 original condition (370 °C) while asphaltenes at RTFO and PAV presented similar decomposition  
3 values and significantly higher than the original condition (378 °C) indicating that the samples had  
4 high stability specially below 200 °C.

5 The test results evidenced that maltenes were also highly stable below 200 °C, however, the  
6 mass loss was significantly higher at any aging stage than the asphaltenes. This behavior can be  
7 attributed to volatilization or evaporation of the lighter components found in the maltenes. Another  
8 significant finding was observed for the decomposition temperature of the maltenes which was  
9 about 8% lower than the asphaltenes.

10



11

12

**FIGURE 4 Thermo gravimetric analysis (a) asphaltenes, (b) maltenes.**

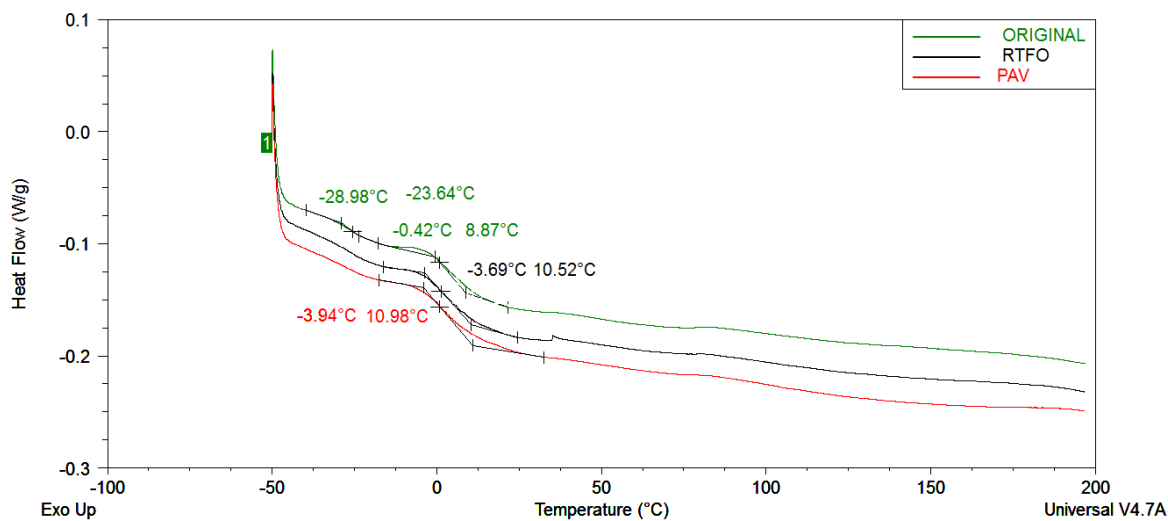
13



## 1 DIFFERENTIAL SCANNING CALORIMETRY ANALYSIS

2 DSC is widely used for determination of thermal transitions brought about by the first order  
3 transitions, such as melting and crystallization of crystallizable species (11). Glass transition,  $T_g$ ,  
4 credited as a second order phenomenon taking place in the amorphous region of the sample, can be  
5 also defined by DSC, but it depends largely on the nature of the material and its content of  
6 crystallizable fractions. Below the glass transition temperature, asphalt behaves like a glass and  
7 appears brittle.

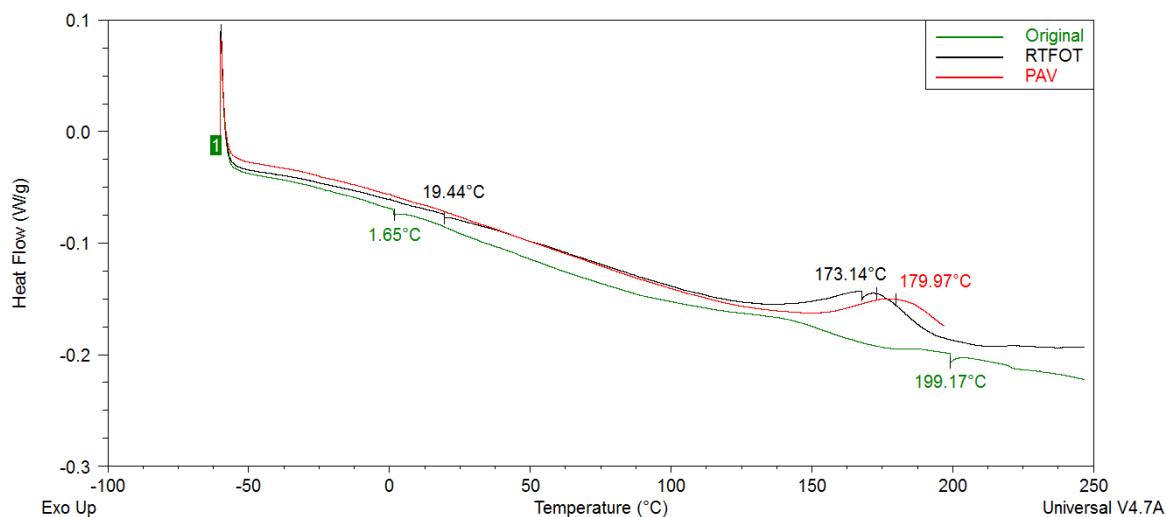
8 DSC analysis was performed to observe sample behavior due to the change on temperature  
9 in a range from  $-50^{\circ}\text{C}$  up to  $200^{\circ}\text{C}$ . Based on the data collected by the DSC analysis, the glass  
10 transition temperature ( $T_g$ ) was determined when possible. Figure 5 shows how the original asphalt  
11 presents a couple of secondary transition (softening) zones between  $-28$  and  $-23^{\circ}\text{C}$  and  $-0.4$  and  $8.9$   
12  $^{\circ}\text{C}$  due to molecular rearrangement. For the RTFO and PAV stages, secondary transition zones were  
13 found at significantly higher temperatures compared to the unaged stage, however, between RTFO  
14 and PAV the temperature range for these zones was not significantly different.



17  
18 **FIGURE 5 DSC Analysis of original asphalt.**

19  
20 When analyzing the asphaltenes at the unaged and RTFO stages an endothermic behavior was  
21 observed at  $1.6$  and  $19.4^{\circ}\text{C}$  due to molecular rearrangement (Figure 6). On the other hand, an  
22 exothermic phenomenon, similar to crystallization, was observed for the RTFO and PAV stages of  
23 the asphaltenes at high temperatures also due to molecular rearrangement. This behavior could be  
24 correlated to the Superpave intermediate performance temperatures and could help explain fatigue  
25 cracking performance.

26 Maltenes were the only samples that showed glassy transitions as illustrated in Figure 7. In  
27 the unaged stage the glassy temperature ( $T_g$ ) was found to be between  $-4.5$  and  $4.9^{\circ}\text{C}$  while at the  
28 RTFO the  $T_g$  ranged from  $-24.7$  to  $-21.5^{\circ}\text{C}$  and it became even lower at the PAV stage with values  
29 between  $-35.8$  to  $-26.12^{\circ}\text{C}$ . A decrease in the  $T_g$  values as the aging of the maltenes increases  
30 explains the unexpected decrease in the complex shear modulus because, as observed with the DSC  
31 analysis, aged maltenes tended to flow (became softer) at lower temperatures.  
32



1

2

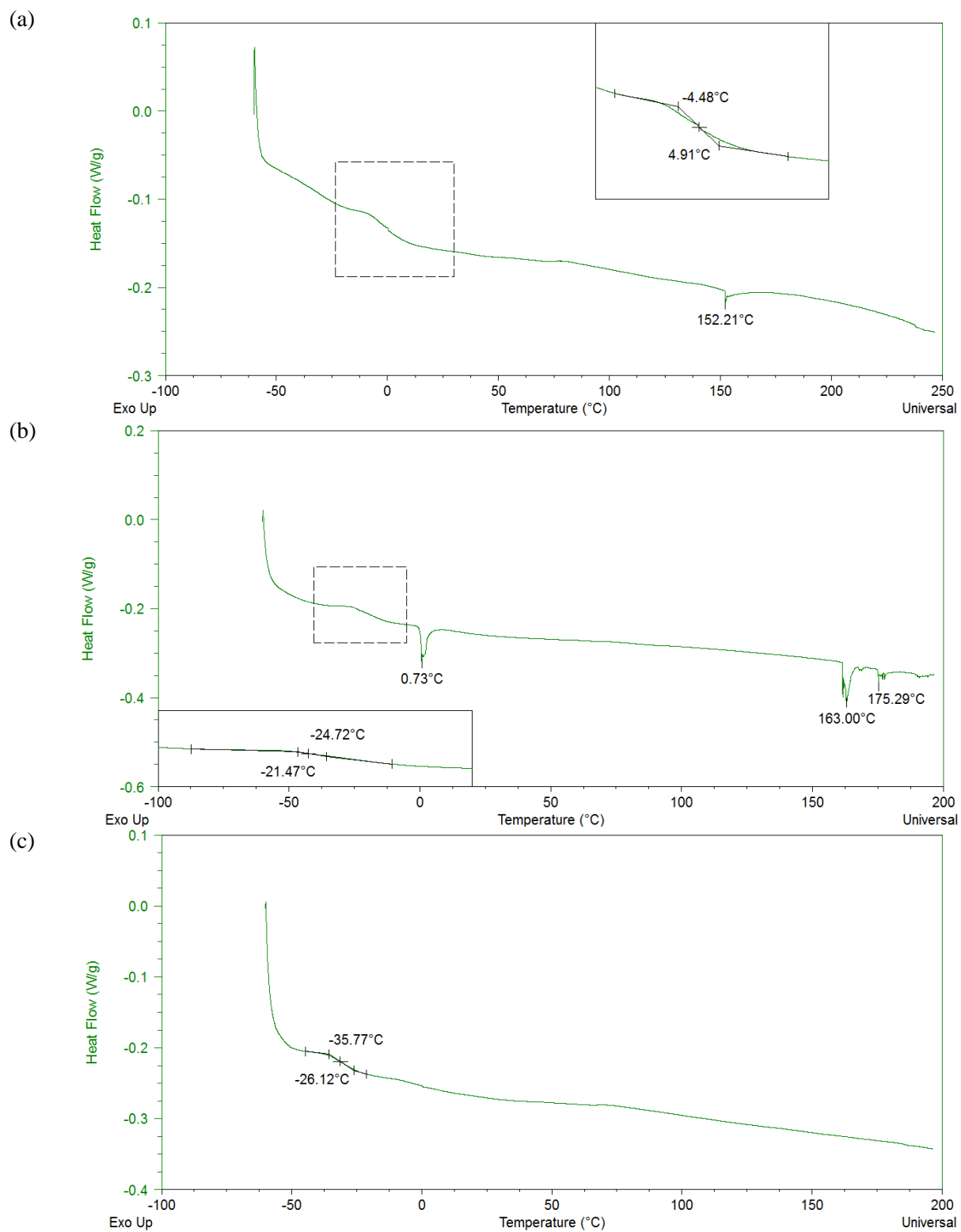
**FIGURE 6 DSC Analysis of asphaltenes.**

3

#### 4 **FOURIER TRANSFORM INFRARED SPECTROSCOPY ANALYSIS**

5 FTIR is a technique used to identify and quantify amounts of known and unknown materials (12).  
6 In this technique, infrared radiation is passed through a sample; some of this radiation is absorbed  
7 by the sample and some of it is passed through (transmitted). The resulting spectrum represents the  
8 molecular absorption and transmission, creating a molecular fingerprint of the sample (13-15).

9 Figure 8 shows the FTIR spectrums for the binder and its two studied components at the unaged  
10 stage. The characteristic bands for the different phases were summarized on Table 3. The  
11 differences in the singular components of the asphalt binder are highlighted with respect to the neat  
12 asphalt binder. The asphaltenes correspond to a large fraction of complex polar aromatic  
13 compounds that are highly insoluble in paraffinic solvents such as *n*-heptane and are solid at room  
14 temperature. Because of the type of interactions they present bands typical of the asphalt binder.  
15 Additionally, because of the separation process, the sample may be contaminated with other phases  
16 due to the strong interactions with other components.  
17



1

2

**FIGURE 7 DSC Analysis of maltenes (a) original, (b) RTFO, (c) PAV.**

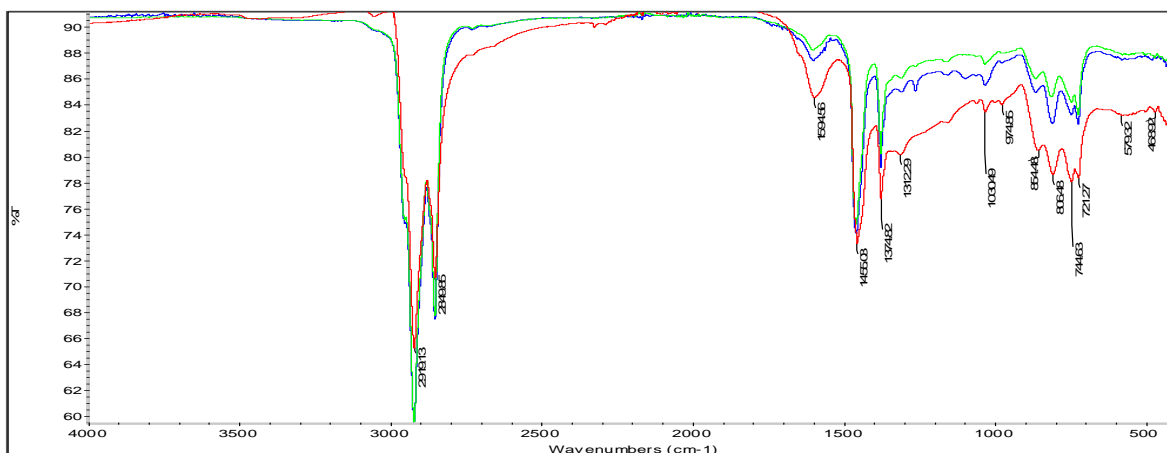


FIGURE 8 FTIR analysis of unaged samples. (Blue = binder, Red = asphaltenes, Green = maltenes).

TABLE 3 FTIR Analysis of unaged samples

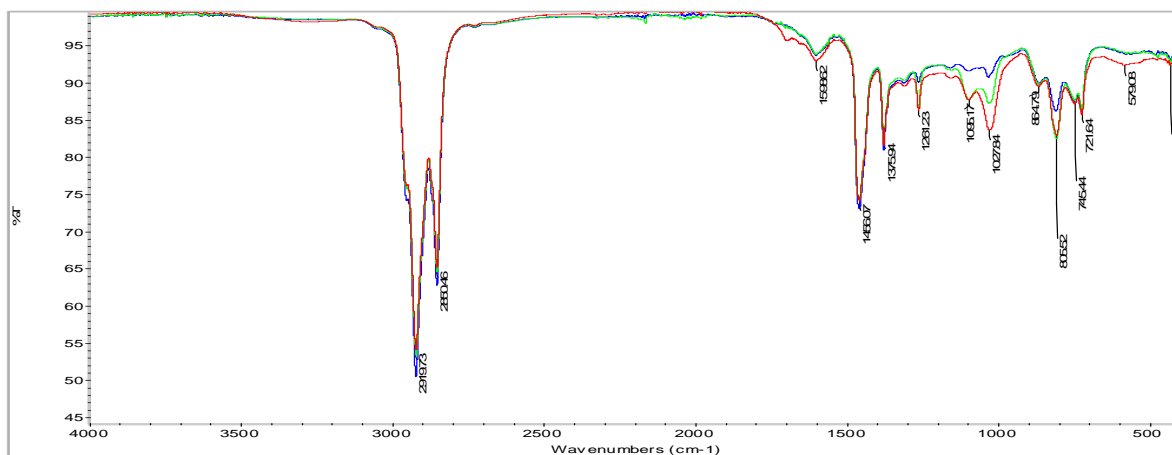
| Wavelength (cm <sup>-1</sup> ) | Asphalt Binder  | Asphaltenes   | Maltenes   |
|--------------------------------|---|---|--|
| 2851- 2920                     | High intensity band of CH <sub>2</sub> and CH <sub>3</sub> groups ( <i>Saturated hydrocarbons</i> )   | High intensity band of CH <sub>2</sub> and CH <sub>3</sub> groups ( <i>Saturated hydrocarbons</i> )   | High intensity band of CH <sub>2</sub> and CH <sub>3</sub> groups ( <i>Saturated hydrocarbons</i> )  |
| 1600                           | Low intensity band of C=C (Ar) ( <i>Aromatic hydrocarbons</i> )                                       | Medium intensity band of C=C (Ar) ( <i>Aromatic hydrocarbons</i> ) <b>intensified</b>                 | Low intensity band of C=C (Ar) ( <i>Aromatic hydrocarbons</i> )  |
| 1500                           | Medium intensity band of C=C (Ar) ( <i>Aromatic hydrocarbons</i> )                                    | Medium intensity band of C=C (Ar) ( <i>Aromatic hydrocarbons</i> )                                    | Medium intensity band of C=C (Ar) ( <i>Aromatic hydrocarbons</i> ) <b>Lower intensity - possibly combined with 1460 cm<sup>-1</sup> band</b> |
| 1450                           | Medium intensity band of CH <sub>2</sub> and CH <sub>3</sub> groups ( <i>Saturated hydrocarbons</i> ) | Medium intensity band of CH <sub>2</sub> and CH <sub>3</sub> groups ( <i>Saturated hydrocarbons</i> ) | Medium intensity band of CH <sub>2</sub> and CH <sub>3</sub> groups ( <i>Saturated hydrocarbons</i> )  |
| 1340                           | Medium intensity band of C-N ( <i>Aromatic Amines</i> )   | Medium intensity band of C-N ( <i>Aromatic Amines</i> )   | Medium intensity band of C-N ( <i>Aromatic Amines</i> )  |
| 1170                           | Low intensity band of R-O-Ar ( <i>Alkyl aryl ethers</i> )   | Low intensity band of R-O-Ar ( <i>Alkyl aryl ethers</i> )   | Low intensity band of R-O-Ar ( <i>Alkyl aryl ethers</i> )  |
| 1030                           | Low intensity band of R-O-Ar ( <i>Alkyl aryl ethers</i> )   | Low intensity band of R-O-Ar ( <i>Alkyl aryl ethers</i> )   | Low intensity band of R-O-Ar ( <i>Alkyl aryl ethers</i> )  |
| 750                            | Low intensity band of C-H meta ( <i>Aromatic compounds</i> )  | Low intensity band of C-H meta ( <i>Aromatic compounds</i> ) <b>lower intensity</b>                   | Low intensity band of C-H meta ( <i>Aromatic compounds</i> ) <b>Higher intensity</b>   |
| 720                            | Low intensity band of C-H para ( <i>Aromatic compounds</i> )  | Low intensity band of C-H para ( <i>Aromatic compounds</i> ) <b>lower intensity</b>                   | Low intensity band of C-H para ( <i>Aromatic compounds</i> ) <b>Higher intensity</b>   |

(\*) The comments in **bold** are with respect to the neat asphalt binder.

The asphalt binder presented physical and chemical changes when subjected to a thermal oxidative process. This can be caused by the loss of volatiles or specimens of low molecular weight, or even by the formation of hydrogen bonds. The groups typically formed asphalt binders upon aging are carboxylic acids (-COOH), ketones (C-CO-C), sulfoxides (R-SO-R) and anhydrides (C-O-C) (16). These oxidation products form polar groups with strong interaction increasing viscosity and changing flow properties. An increase in the intensity and appearance of different bands from 805 to 1260 cm<sup>-1</sup> due to oxidation (anhydrides) can be seen in Figure 9. The characteristic bands for the two aging conditions were summarized on Tables 5 and 6 for the binder and its individual

1 components. Evidence of asphaltenes and maltenes oxidation was only present for the PAV samples  
 2 at  $1700\text{ cm}^{-1}$  which relates directly to oxygen content (17). On the other hand there was a small  
 3 change in the intensity of different bands from  $805$  to  $1260\text{ cm}^{-1}$  that could be related to oxidation  
 4 for maltenes at RTFO and PAV conditions.

5



6

7 **FIGURE 9 FTIR Analysis of the asphalt binder. (Blue = unaged, Green = RTFO, Red =**  
 8 **PAV).**

9

10 **TABLE 4 FTIR Analysis of RTFO samples**

| Wavelength (cm <sup>-1</sup> ) | Binder  | Asphaltenes   | Maltenes   |
|--------------------------------|---|---|--|
| 1600                           | -   | Medium intensity band of C=C (Ar) (Aromatic hydrocarbons) <b>intensified</b>                                      | Low intensity band of C=C (Ar) (Aromatic hydrocarbons) <b>Highly reduced</b> |
| 1500                           | -   | Medium intensity band of C=C (Ar) (Aromatic hydrocarbons) <b>possibly combined with 1460 cm<sup>-1</sup> band</b> | -  |
| 1260                           | Low intensity band of R-N-O Nitrogen oxidation <b>New band</b>                | Medium intensity band of R-N-O  | Medium intensity band of R-N-O. <b>Not present</b>                           |
| 1070                           | Low intensity band of R-O-R (ethers) <b>New band</b>                          | -   | -  |
| 1030                           | Low intensity band of R-O-Ar (Alkyl aryl ethers) <b>Significant Increment</b> | Low intensity band of R-O-Ar (Alkyl aryl ethers)  | Low intensity band of R-O-Ar (Alkyl aryl ethers)                             |
| 805                            | Medium intensity band of C-H meta <b>Significant Increment</b>                | -   | -  |

11 (\*) The comments in **bold** are changes with respect to the unaged samples.

12

13

14

15

1 **TABLE 5 FTIR analysis of PAV samples**

| Wavelength (cm <sup>-1</sup> ) | Neat Asphalt Binder  | Asphaltenes  | Maltenes   |
|--------------------------------|--|--|--|
| 1700                           | Low intensity band of RRC=O (carbonyls)<br><b>New band</b>                       | Low intensity band of RRC=O (carbonyls)<br><b>New band</b>   | Low intensity band of RRC=O (carbonyls)<br><b>New band</b>                             |
| 1600                           | -  | Medium intensity band of C=C (Ar) (Aromatic hydrocarbons)<br><b>intensified</b>                                  | Low intensity band of C=C (Ar) (Aromatic hydrocarbons)<br><b>Significant reduction</b> |
| 1500                           | -  | Medium intensity band of C=C (Ar) (Aromatic hydrocarbons)<br><b>Increment</b>                                    | Medium intensity band of C=C (Ar) (Aromatic hydrocarbons)<br><b>Not Present</b>        |
| 1450                           | -  | Medium intensity band of CH <sub>2</sub> and CH <sub>3</sub> groups (Saturated hydrocarbons)<br><b>Increment</b> | -  |
| 1340                           | -  | -  | Medium intensity band of C-N (Aromatic Amines)<br><b>Significant reduction</b>         |
| 1260                           | Low intensity band of R-N-O Nitrogen oxidation<br><b>Higher intensity</b>        | Medium intensity band of R-N-O<br><b>Not present</b>   | Medium intensity band of R-N-O.<br><b>Not present</b>                                  |
| 1170                           | -  | -  | Low intensity band of R-O-Ar (Alkyl aryl ethers)<br><b>Not present</b>                 |
| 1070                           | Low intensity band of R-O-R (ethers)<br><b>New band</b>                          | Low intensity band of R-O-R (ethers)<br><b>New band</b>  | -  |
| 1030                           | Low intensity band of R-O-Ar (Alkyl aryl ethers)<br><b>Significant increment</b> | Low intensity band of R-O-Ar (Alkyl aryl ethers)<br><b>Significant increment</b>                                 | Low intensity band of R-O-Ar (Alkyl aryl ethers)<br><b>Significant reduction</b>       |
| 805                            | Medium intensity band of C-H meta<br><b>Significant Increment</b>                | Medium intensity band of C-H meta<br><b>Significant Increment</b>  | -  |
| 750                            | -  | -  | Low intensity band of C-H meta (Aromatic compounds)<br><b>Decreased</b>                |
| 720                            | -  | -  | Low intensity band of C-H para (Aromatic compounds)<br><b>Decreased</b>                |

2 (\*) The comments in **bold** are changes with respect to the unaged samples.

3  
4 **CONCLUSIONS**

5  
6 Based on the results of this study the following conclusions were reached:

- 7
- 8 • At intermediate temperatures asphaltenes account for the majority of the elastic component of the complex shear modulus of the asphalt binder while maltenes account for the majority of the viscous component. However, at high temperatures it is not clear which component is responsible for either the elastic or viscous behavior of the binder.
  - 9 • With aging, the amount of asphaltenes in the binder showed the lowest change in composition (highest stability) followed by the saturated fraction while the composition of aromatics and resins seemed to interchange with each other.
  - 10 • Polarized Light Microscopy is a simple technique that can be implemented to help explain changes in stress states or changes in composition of bituminous materials. This technique provided evidence that some of the resins and oils were transformed into asphaltene-like substances due to aging.
  - 11 • Thermal stability of the asphalt binder can be attributed mostly to the higher stability of the asphaltenes at normal handling temperatures of the asphalt (below 200 °C).
  - 12 • For the RTFO and PAV conditions, secondary transition zones were found at significantly higher temperatures (close to ambient temperatures) compared to the unaged stage that could be correlated to the Superpave intermediate performance temperatures and could help explain fatigue cracking performance.
- 13  
14  
15  
16  
17  
18  
19  
20  
21  
22  
23

- 1 • With aging, the thermodynamic behavior of the maltenes, as demonstrated by their glassy  
2 transition behavior, was directly correlated to their rheological performance.
- 3 • The higher stability of asphaltenes is responsible for the lower change in composition as  
4 observed by the Iatroskan Thin Film Chromatography analysis, and also responsible for the  
5 lower susceptibility to oxidation.
- 6 • Overall, there is clear evidence that aging of the asphalt binder components has an effect on  
7 the morphology of the asphalt binder.

## 10 REFERENCES

- 11 1. Roberts, F. L., Kandhal, P. S., Brown, E. R., Lee, D., and Kennedy, T. W. *Hot mix asphalt*  
12 *materials, mixture design, and construction*, 2nd Ed., Napa Education Foundation, Lanham,  
13 Md. 1996.
- 14 2. Nellensteyn, F.J. *Relation of the Micelle to the Medium in Asphalt*. Journal of the institute  
15 of Petroleum Technologist, Vol. 14, 1928.
- 16 3. Traxler, R. N., *Asphalt: Its Composition, Properties, and Uses*. Reinhold, NY. 1961.
- 17 4. Whiteoak, C.D., *The Shell Bitumen Handbook*, Shell Bitumen, U.K, 1990.
- 18 5. Pink, H.S., Merz, R.E., and Bosniak, D.S. (1980), *Asphalt Rheology: Experimental*  
19 *Determination of Dynamic Moduli at Low Temperature*, Proceedings of the  
20 Association of Asphalt Paving Technologists, volume 49, p.64.
- 21 6. Asphalt Institute. *The asphalt handbook*. Manual Series No. 4 (MS-4), The Asphalt  
22 Institute, Lexington, KY., 1989.
- 23 7. Bahia, H. U. and D. A. Anderson. *Glass Transition Behavior and Physical Hardening of*  
24 *Asphalt Binders*. Journal of the Association of Asphalt Paving Technologists, Vol. 62, 93-  
25 129. 1993.
- 26 8. Allen, R.G., *Structural characterization of micromechanical Properties in asphalt using*  
27 *atomic force microscopy*. M.Sc. Thesis. College Station, TX. 2010.
- 28 9. Gustav J., *Essentials of Polarized Light Microscopy*, College of Microscopy, Fifth Edition,  
29 January 2008.
- 30 10. Coats, A. W.; Redfern, J. P., *Thermogravimetric Analysis: A Review*. Analyst 88: 906–924.  
31 1963.
- 32 11. Elseifi, M., Mohammad, L.N., Glover, I., Negulescu, I., Daly, W.H., and Abadie,  
33 C., *Relationship between Molecular Compositions and Rheological Properties of Neat*  
34 *Asphalt Binder at Low and Intermediate Temperatures*, Journal of Materials in Civil  
35 Engineering, 2010.
- 36 12. Marasteanu, M., R. Velasquez, W. Herb, J. Tweet, M. Turos, M. Watson and H. Stefan.  
37 *Determination of Optimum Time for the Application of Surface Treatments to Asphalt*  
38 *Concrete Pavements—Phase II*. Final Report No. MN/RC 2008-16, Minnesota Dept. of  
39 Transportation, St. Paul, MN, 2008.
- 40 13. Thermo Nicolet Corporation. *Introduction to Fourier Transform Infrared Spectroscopy*.  
41 2001.
- 42 14. Daly, W. H., I. Negulescu, and I. A. Glover. *Comparative Analysis of Modified Binders:*  
43 *Original Asphalts and Materials Extracted from Existing Pavements*. Federal Highway  
44 Administration Report No. FHWA/LA.10/462. Baton Rouge, LA, 2010.
- 45 15. Kuptsov, A.H. *Applications of Fourier Transform Raman Spectroscopy in Forensic*  
46 *Science*. Journal of Forensic Sciences, JFSCA, Vol. 39, No. 2, pp. 305-318. 1994.
- 47 16. J. F. Masson, L. Pelletier, P. Collins, *Rapid FTIR method for quantification of styrene-*  
48 *butadiene type copolymers in bitumen*. Journal of Applied Polymer Science 79, 1034 –  
49 1041. 2001.

- 1        17. Lu, X., and U. Isacson, *Chemical and Rheological Evaluation of Ageing Properties of*
- 2                *SBS Polymer Modified Bitumens*, Fuel, 77(9/10), 961, 1998.